Electronic Supplementary Information (ESI) for

Sailing towards sustainability: offshore wind's green hydrogen potential for decarbonization in coastal USA

Authors: Rishi Kaashyap Balaji[a], Fengqi You[*abc]

Affiliations:

[a] Systems Engineering, College of Engineering, Cornell University, Ithaca, New York 14853, USA.

[b] Robert Frederick Smith School of Chemical and Biomolecular Engineering, Cornell University, Ithaca, New York 14853, USA.

[c] Cornell Atkinson Center for Sustainability, Cornell University, Ithaca, New York 14853, USA.

This document contains:

- Supplementary text
- Supplementary notes S1, S2, S3, S4
- Supplementary figures S1, S2
- Tables S1, S2, S3, S4

[*] Corresponding author. Phone: (607) 255-1162; Fax: (607) 255-9166; E-mail: fengqi.you@cornell.edu

Supplementary Information Text

This supplementary document provides a detailed account of the five demand scenarios considered in the study as outlined in the section **Methods, Hydrogen demand** and describes the supplementary results of the delivered cost estimates obtained from all these scenarios, building on the discussion in the section **Results, Delivered costs of hydrogen produced offshore**. Further, it also provides a detailed account on the development of optimization models P1 and P2 for the design of offshore wind-to-hydrogen facilities. The primary role of the outlined optimization models is to identify design parameters at the system and sub-system levels, thereby serving as the basis for the techno-economic analysis of hydrogen delivery costs and supplying inputs for the life cycle assessments. The models involve decisions in two distinct stages. The investment stage determines the facility location and sizes of the subsystems, while the operational stage defines time-varying operating levels for each subsystem. The study delves into four distinct scenarios, as outlined in the section **Methods, Multi-scale systems analysis**, which center around state-level and hub-level evaluations of two delivery pathways: compressed gaseous hydrogen pipelines and liquefied hydrogen shipping. These are the two direct hydrogen transport forms that do not involve the interconversion of hydrogen to hydrogen carriers.

To ensure a nuanced understanding, the delivery pathways are analyzed through independent models which can be applied at both the state-level and hub-level for all the demand scenarios. While all facilities are assumed to be located along the midpoint of the exclusive economic zone (EEZ) and will have a uniform distance to the coast in the state-wise scenarios, in the hub-wise scenarios as there is just one facility per hub, the distances between the central facility and states change. The approach of analyzing the delivery scenarios separately recognizes the interest and varied applicability of the two different direct hydrogen transport technologies for offshore wind-to-hydrogen systems under different levels of demands aiming to provide a holistic perspective. As the model is largely robust to distance changes within the EEZ due to minimal cost contribution of pipelines to the delivered costs and the round-trip time based approach used for liquefied hydrogen shipping route, these scenarios based on these variations are not explicitly studied.

Following the discussion on demand scenarios and corresponding supplementary results in note S1, we provide a nomenclature section introducing key parameters and decision variables, and subsequently proceed to articulate the optimization problem formulations in notes S2 and S3, describing objectives and constraints. Additionally, readers are directed to references that elucidate the solution techniques and algorithms applied in solving these models.

S1. Demand Scenarios

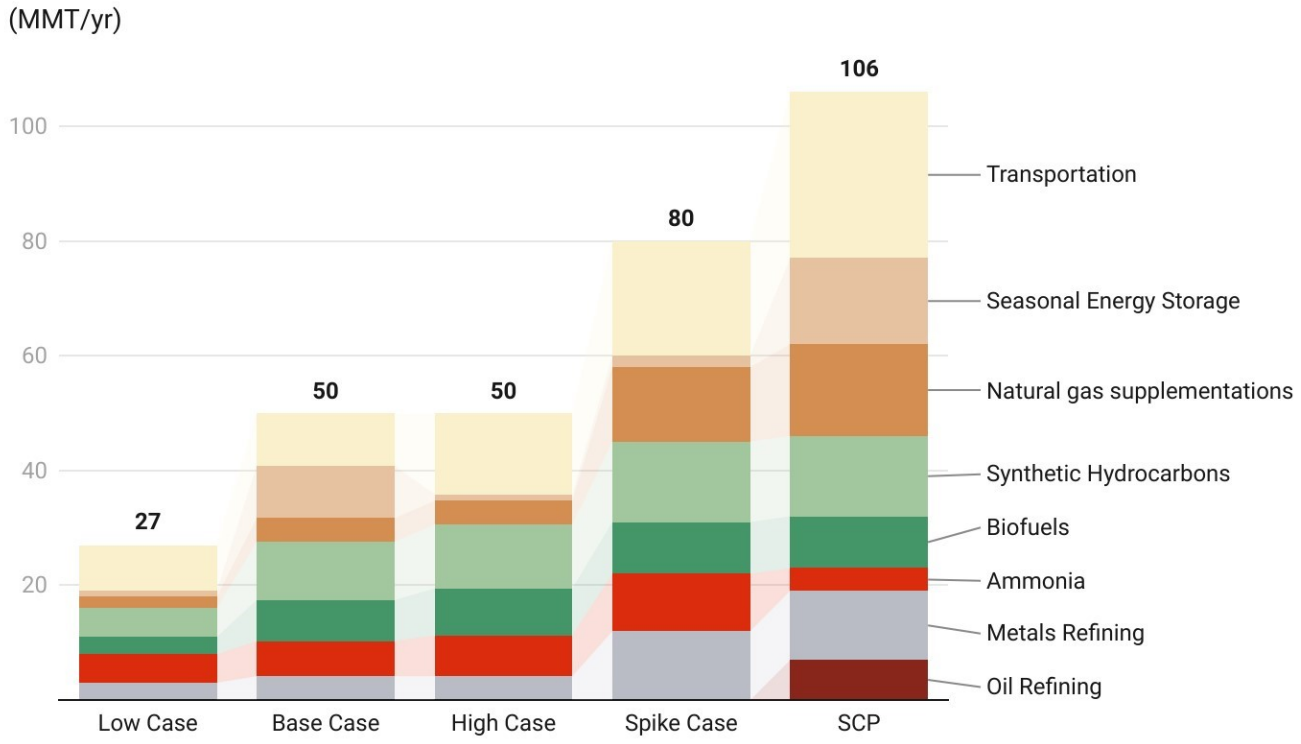

Figure S1. Scenarios for Hydrogen Demand in USA for 2050

In the report, 'Pathways to Commercial Liftoff: Clean Hydrogen'[1], the U.S. Department of Energy outlines a phased evolution for the U.S. hydrogen market over the next few decades, projecting a series of stages characterized by the emergence of new end-uses, the growth of domestic demand, and the expansion of infrastructure. These phases are described as near-term expansion, industrial scaling, and long-term growth. The department forecasts that the long-term growth phase will commence in 2035, with the hydrogen market reaching a mature state by 2050, a critical milestone in achieving net-zero emissions. Given that factors such as availability, price, ease of adoption, and competition with other technologies, influence the evolving applications of hydrogen for decarbonization and the commercial uptake is in still in nascent forms, this evolution could have different outcomes leading to different hydrogen demand scenarios in 2050, as depicted in Figure S1. Table S1 further enumerates the numerical contributions at the sectoral level for each of these scenarios.

This study considers the five demand scenarios outlined in Fig, S1 for analysis of the delivered costs and lifecycle GHG emissions of green hydrogen produced offshore in 2050. The serviceable consumption potential (SCP) estimated by the National Renewable Energy Lab for 2050[2], is treated as the most optimistic scenario, representing the upper bound of hydrogen market size. Hence, this scenario is used as a limiting case to assess the adequacy of offshore wind resources for green hydrogen production and to obtain the best estimates of cost,

considering the most significant effect from economies of scale. Since state-level data is also available only for the SCP scenario[3], it is used as the basis for deriving state-level demand data for other scenarios, assuming that the percentage sectoral contributions from each state remain constant across all scenarios. Additionally, as shown in Figure S2, the analysis indicates that the sensitivity of delivered cost estimates to changes in demand across these scenarios, for both delivery pathways and configurations at both state and hub levels, is limited across all states. In most cases, this variation is limited to less than \$0.25/kg H_2 across the Low Case and the SCP Case which represent the lowest and highest demand forecasts respectively. While the price sensitivity may remain limited, the uncertainty in demand evolution poses a challenge to investment decisions and policy measures are required to ensure that the supply and demand grow in synchronization.

Table S1. Sectoral contributions to the hydrogen demand in 2050 for the five demand scenarios

Sector	**Low Case[1, 4]**	**Base Case[1, 4]**	**High Case[1, 4]**	**Spike Case[1]**	**Serviceable Consumption Potential Case (SCP)** [2]
Oil Refining	-	-	-	-	7.00
Metals Refining	3.0	4.14	4.14	12.00	12.00
Ammonia	5.00	6.14	7.14	10.00	4.00
Biofuels	3.00	7.14	8.14	9.00	9.00
Synthetic Hydrocarbons	5.00	10.14	11.14	14.00	14.00
Natural gas supplementations	2.00	4.14	4.14	13.00	16.00
Seasonal Energy Storage	1.00	9.14	1.14	2.00	15.00
Transportation	8.00	9.14	14.14	20.00	29.00
Total	**27.00**	**50.00**	**50.00**	**80.00**	**106.00**

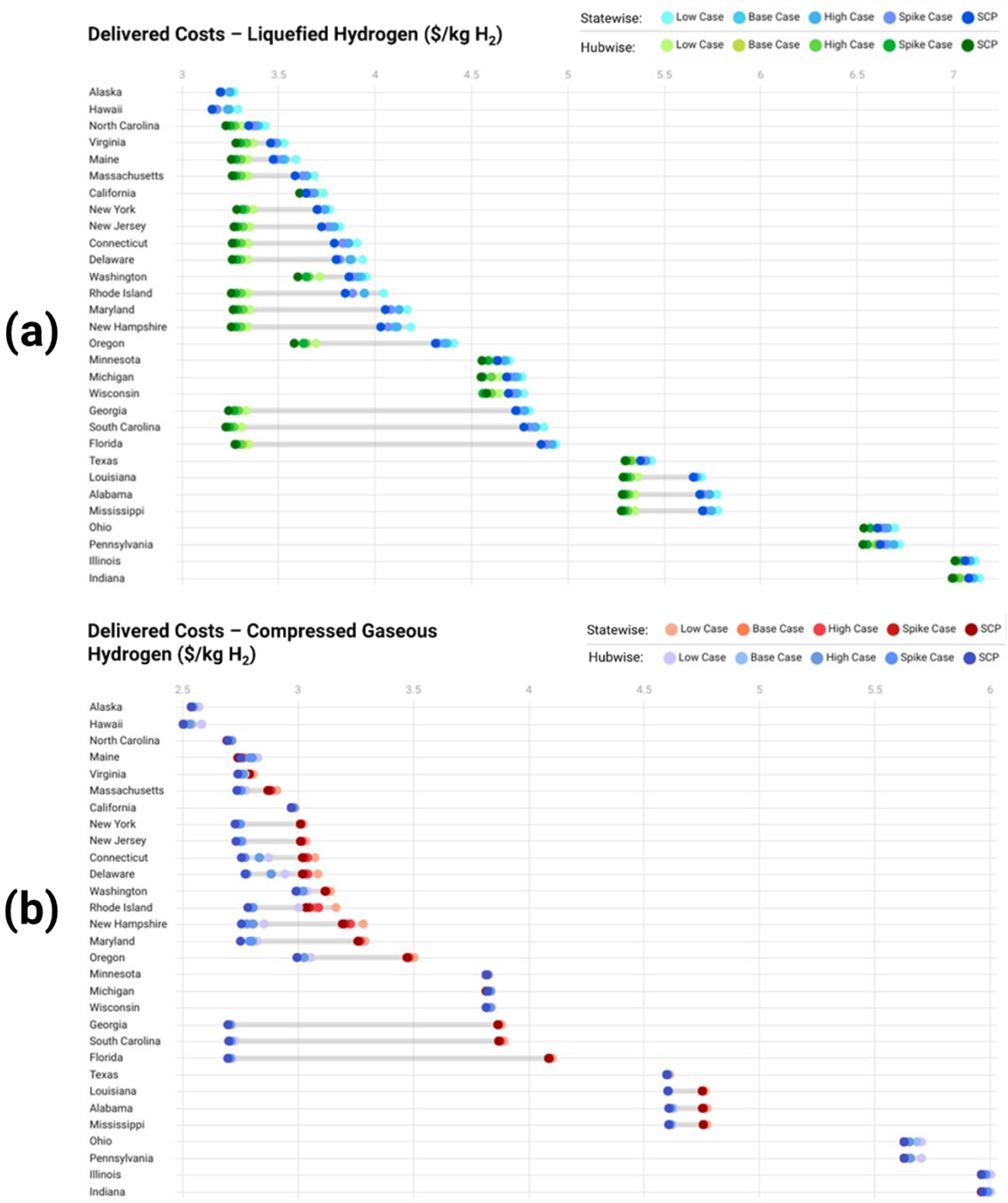

Figure S2. (a) The delivered costs of liquified hydrogen shipping pathway (b) the delivered costs of the compressed gaseous hydrogen pathway for the five scenarios for Hydrogen Demand in USA for 2050

Nomenclature

Indices, Subscripts & Superscripts

Comp	Compression
d	Demand location
D	Set of Demand Locations
DES	Desalination
EL	Electrolysis
f	Facility
F	Set of Candidate Facility Locations
FLP	Floating Platform
i	Ship Type
LIQ	Liquefaction
Pipe	Pipelines
Pump	Pumping
S	Shipping
STO	Storage
t	Time Period
T	Set of Time periods
TRA	Transport
WT	Wind Turbines

Parameters

a, b, c, d	Coefficients for annualized pipeline cost estimation based on HDSAM Equation
$A^{L,EL}$	Area of Electrolytic Hydrogen Production Plant per GW of Electrolyzer Capacity
BO	Boil-off rate of liquefied hydrogen
CF_t^f	Capacity factor for offshore wind energy generation
C_i^S	Capacity of ship of type *i*
h^m	Height of wind speed measurements
h^t	Hub height of offshore wind turbine
$L^{f,d}$	Length of pipeline from facility *f* to demand location *d*
M	Big-M constant
N^{Days}	Number of days in a representative calendar year

$\left(\frac{\Delta P}{l}\right)$	Pressure drop per unit length in hydrogen pipeline
$P_i^{S,TRA}$	Transportation cost per round trip for ship of type i
$RTT^{f,d}$	Round Trip Time between facility f and demand location d in days
TAC^x	Total annualized cost of sub-system x
$v^{w,co}$	Cut-off speed for wind turbine
$v^{w,ci}$	Cut-in speed for wind turbine
$v^{w,r}$	Rated speed for wind turbine
$V^{\max}$	Maximum permissible design velocity of hydrogen in pipelines
W^{Des}	Water desalinated per unit mass of hydrogen produced
ρ^{H_2}	Density of hydrogen at 700 Bar
η^{EL}	Efficiency of electrolysis
Φ^{Comp}	Energy consumed for compression per MT of H_2
Φ^{Des}	Energy consumed for desalination per unit volume of water processed
Φ^{EL}	Energy consumed for electrolysis per MT of H_2 produced
Φ^{LIQ}	Energy consumed for liquefaction per MT of H_2
Φ^{WT}	Nominal energy generation capacity from wind turbines in a day
θ^L	Scaling factor for the cost of liquefaction
θ^S	Scaling factor for the cost of liquified hydrogen storage
θ^C	Scaling factor for the cost of compression
θ^P	Scaling factor for the cost of pumping
θ^{Pipe}	Scaling factor for the cost of pipelines in the HDSAM equation

Decision variables

$A^{f,d,pipe}$	Cross sectional area of H_2 pipeline from facility f to demand location d
$C^{f,x}$	Installed capacity of subsystem x at facility f
$E_t^{f,WT}$	Energy generated by offshore wind turbines at facility f at time period t
$E_t^{f,x}$	Energy consumed by subsystem x at facility f at time period t
$E_t^{f,d,pump}$	Energy consumed in pumping H_2 from facility f to demand location d through pipelines at time period t

F_t^{f,H_2}	Amount of H_2 produced in facility f at time period t
$L_t^{f,STO}$	Mass of H_2 in the storage tank at time t in facility f
M_t^{f,d,H_2}	Mass flow rate of hydrogen from facility f to demand location d at time period t
$N^{f,WT}$	Number of offshore wind turbines installed at facility f
$N_i^{f,S}$	Number of ships of type i purchased at facility f
$NT_i^{f,d}$	Total number of trips in a year between facility f and demand location d of ship type i
$S_{i,t}^{f,d}$	Number of shipments through ship type i from facility f to demand location d at time period t
x^f	Binary facility selection variable for facility f

S2. Model formulation: liquefied hydrogen shipping

This supplementary note presents the model formulation for the problem P1 used for the optimal design of the liquified hydrogen shipping based offshore wind to hydrogen facilities .

The overall optimization problem can be stated as follows. Given a geographically distributed set of demands for hydrogen, a set of candidate offshore locations for siting the offshore wind-to-hydrogen facilities and the associated time varying capacity factor for offshore wind power generation, a set of candidate ports on the coastline to serve as receiving terminals for liquid hydrogen, annualized capital and operational costs of investment in technologies used along the process sequence, capacity of each type of ship, cost of transportation, energy consumption per unit of operation for each process step, ship speed & distance (captured as round trip time); design the overall supply chain by selecting one central production facility per hub, sizing each facility by determining the capacities required for process steps & schedule the overall operations (production, storage & transport to all demand locations) over the span of a representative year such that the total annualized cost of hydrogen delivery through the system is minimized while adhering to the energy balance constraints, capacity constraints, transportation & storage constraints.

The above optimization problem is formulated as a mixed integer non-linear program (MINLP). The mathematical formulation of P1 is as follows:

Objective function

The objective function *obj* shown in Eq. (S1) quantifies total annualized cost (TAC) of hydrogen delivery through the liquified hydrogen shipping based offshore wind to hydrogen facility comprising individual sub-systems such as offshore wind turbines, desalination, electrolysis, liquefaction, storage, and shipping. Individual terms represent the TAC of these subsystems, which are obtained by multiplying their unit TAC values (with

appropriate units) and corresponding capacities. Shipping costs are calculated as a sum of the annualized costs of dedicated shipping fleet purchased for each facility and roundtrip transportation costs for each journey between the offshore facility and the coastal receiving site. Liquefaction and storage costs are subject to non-linear scaling[5], while other subsystem expenses linearly scale based on their installed capacities. The unit TAC of each sub-system was obtained from the CAPEX and OPEX costs (See **Methods, Technology Costs**).

$$\begin{aligned} \text{min:} \quad obj = & \sum_f \left(TAC^{WT} \cdot N^{f,WT} + TAC^{DES} \cdot C^{f,DES} + TAC^{EL} \cdot C^{f,EL} + TAC^{FLP} \cdot A^{L,EL} \cdot C^{f,EL} \right) \\ & + \sum_f \left(+ TAC^{LIQ} \cdot C^{f,LIQ^{\theta^L}} + TAC^{STO} \cdot C^{f,STO^{\theta^S}} \right) \\ & + \sum_f \sum_i TAC_i^S \cdot N_i^{f,S} + \sum_f \sum_d \sum_i NT_i^{f,d} \cdot P_i^{S,TRA} \cdot RTT^{f,d} \end{aligned} \tag{S1}$$

Constraints

Facility selection constraints

The facility selection constraints ensure that a single centralized facility is selected for each hub amongst all the proposed candidate locations. Eq. (S2) uses a binary variable for imposing this restriction, activating only one location in a hub while constraints (S3) – (S9) employ a set of "Big M" constraints[6] using a large positive constant M that ensures the installed capacity of the subsystems are greater than zero only at the location activated for siting in the hub.

$$\sum_f x^f = 1 \tag{S2}$$

$$N^{f,WT} \le M \cdot x^f, \qquad \forall f \in F \tag{S3}$$

$$C^{f,Des} \le M \cdot x^f, \qquad \forall f \in F \tag{S4}$$

$$C^{f,EL} \le M \cdot x^f, \qquad \forall f \in F \tag{S5}$$

$$C^{f,LIQ} \le M \cdot x^f, \qquad \forall f \in F \tag{S6}$$

$$C^{f,STO} \le M \cdot x^f, \qquad \forall f \in F \tag{S7}$$

$$N^{f,S} \le M \cdot x^f, \qquad \forall f \in F \tag{S8}$$

$$\sum_d \sum_i NT_i^{f,d} \le M \cdot x^f, \qquad \forall f \in F \tag{S9}$$

Capacity constraints

The capacity constraints ensure that each of the subsystems, which are operating flexibly by adapting to the variable offshore wind energy generation, remain below their respective installed capacities at each time step. Constraint (S10) pertains to desalination, constraint (S11) to electrolysis, constraint (S12) to liquefaction, and

constraint (S13) to the storage tank. The additional term in Eq. (S13) refers to the boil-off gases which are considered to be re-liquefied along with the primary stream of fresh hydrogen produced through electrolysis.

$$F_t^{f,H_2} \le C^{f,Des}, \qquad \forall f \in F,\ t \in T \tag{S10}$$

$$E_t^{f,EL} \le C^{f,EL}, \qquad \forall f \in F,\ t \in T \tag{S11}$$

$$F_t^{f,H_2} + BO \cdot L_t^{f,STO} \le C^{f,LIQ}, \qquad \forall f \in F,\ t \in T \tag{S12}$$

$$L_t^{f,STO} \le C^{f,STO}, \qquad \forall f \in F,\ t \in T \tag{S13}$$

Energy balance constraints

In this study, the offshore wind-based hydrogen production facilities are treated as isolated energy systems wherein the entire energy output of the offshore wind farm is exclusively channeled into hydrogen production, devoid of additional storage or external supplementation. Thus, Eq. (S14) establishes the energy balance constraint, ensuring that the total energy demand for hydrogen production aligns with the generation from the offshore wind turbines at each time step *t.* As (S14) is an equality constraint, it ensures that all the energy generated in consumed and there is no excess or curtailment to be dealt with through the model. Eq. (S15) quantifies the energy generation at each time step *t* by multiplying the time-varying wind capacity factor specific to the location (See **Methods, Offshore wind energy model**) with the nominal energy output of a single wind turbine, and the total number of installed turbines at facility *f*. Furthermore, Eqs. (S16), (S17), and (S18) fix the energy requirements for desalination, electrolysis, and liquefaction, all of which are energy-consuming processes, based on the hydrogen production level at each time step *t*, unit energy consumption parameters, and assumed process efficiencies.

$$E_t^{f,WT} = E_t^{f,Des} + E_t^{f,EL} + E_t^{f,LIQ}, \qquad \forall f \in F,\ t \in T \tag{S14}$$

$$E_t^{f,WT} = \Phi^{WT} \cdot CF_t^{f} \cdot N^{f,WT}, \qquad \forall f \in F,\ t \in T \tag{S15}$$

$$E_t^{f,Des} = \Phi^{Des} \cdot W^{Des} \cdot F_t^{f,H_2}, \qquad \forall f \in F,\ t \in T \tag{S16}$$

$$E_t^{f,EL} = \frac{\Phi^{EL} \cdot F_t^{f,H_2}}{\eta^{EL}}, \qquad \forall f \in F,\ t \in T \tag{S17}$$

$$E_t^{f,LIQ} = \Phi^{LIQ} \cdot \left(F_t^{f,H_2} + BO \cdot L_t^{f,STO}\right), \qquad \forall f \in F,\ t \in T \tag{S18}$$

Transportation & inventory constraints

Eq. (S19) applies a dynamic material balance on the storage tank, defining the inventory profile over time. The storage tank receives inputs from the upstream production processes and outputs liquified hydrogen to ships. The shipped volume is obtained from multiplying the integer decision variable $S_{i,t}^{f,d}$, which represents the number of full shipments made from facility *f* to demand location *d* for a ship type *i* at each time step *t*, with

C_i^S, the capacity of ship type *i*. These ship types differ based on their hydrogen carrying capacity, with three sizes considered in this study to represent the range of liquefied hydrogen cargo ships that are currently in use and are expected to be purpose-built in the near future catering to requirements for liquified hydrogen shipping[1]. Further, a variation of Eq. (S19) is applied at time-step 0, the by replacing term $L_{t-1}^{f,STO}$ with $L_{364}^{f,STO}$, essentially serving as a cyclicity constraint that enables modeling operating levels across years using a representative 365 day time period[7].

$$L_t^{f,STO} = L_{t-1}^{f,STO} + F_t^{f,H_2} - \sum_d \sum_i S_{i,t}^{f,d} \cdot C_i^S, \qquad \forall f \in F,\ t \in T \tag{S19}$$

Constraints (S20) - (S23) pertain to the transport of liquified hydrogen utilizing a mixed fleet of ships. Constraint (S20) stipulates that for possible roundtrip interval in the planning horizon for every facility-demand location pair, there cannot be more than $N_i^{f,S}$ shipments within the roundtrip duration of each ship. Here, $N_i^{f,S}$ represents the total number of ships of type *i* available in the shipping fleet of facility *f*. Constraint (S21) ensures that a shipment can be scheduled in a given time period only if the level of H_2 in the tank in the previous time step is higher than the total shipment size. Similar to Eq. (S19), a circularity constraint is applied for time step 0 by replacing the term $L_{t-1}^{f,STO}$ with $L_{364}^{f,STO}$ using constraints (S21). Eq. (S22) defines $NT_i^{f,d}$ as the total number of trips taken by ship type *i* to a given demand location *d*, which is equal to the sum of shipments over time. Finally, constraint (S23) restricts the total number of trip days for the shipping fleet associated with facility *f* to be less than or equal to the total number of days in a year times the total number of ships in the fleet of the facility.

$$\sum_d \sum_{t}^{t+RTT^{f,d}} S_{i,t}^{f,d} \le N_i^{f,S}, \qquad \forall f \in F,\ i \in I \tag{S20}$$

$$\sum_d \sum_i S_{i,t}^{f,d} \cdot C_i^{f,S} \le L_{t-1}^{f,STO}, \qquad \forall f \in F,\ t \in T \tag{S21}$$

$$\sum_t S_{i,t}^{f,d} \le NT_i^{f,d}, \quad \forall f \in F,\ i \in I,\ d \in D \tag{S22}$$

$$\sum_d \sum_i \left(NT_i^{f,d} \cdot RTT^{f,d} \right) \le N^{Days} \cdot N_i^{f,S}, \qquad \forall f \in F,\ i \in I \tag{S23}$$

Demand constraint

The demand satisfaction constraint stipulates that the total hydrogen shipped from all active facilities through various ship types must be greater than the demand at each receiving coastal location, ensuring adequate supply to meet the specified requirements. Constraint (S24) stipulates that the demand must be met despite losses of hydrogen that occur during the transportation of the liquid hydrogen due to boil-off.

$$\sum_{f}\sum_{i}\left(NT_i^{f,d}\cdot C_i^S(1-BO)^{0.5\cdot RTT^{f,d}}\right)\geq Demand^d,\qquad \forall\ d\in D \tag{S24}$$

Using the above model, the decisions made through optimization include selecting suitable locations for siting the offshore hydrogen production facilities, sizing facilities and subsystems, scheduling hydrogen production based on daily wind capacity factors, choosing a mixed fleet of ships for each facility, and determining the transport schedules from production facilities to ports. The presence of binary and integer decision variables and two non-linear terms in the objective function, which are concave and are associated with the installed capacity of liquefaction and storage make this model a non-convex MINLP. For the state-level implementation, P1 contains 3662 variables (2559 continuous & 1103 integer) and 4033 constraints.

S3. Model formulation: compressed gaseous hydrogen pipelines

This supplementary note presents the model formulation for the problem P2 used for the optimal design of the compressed gaseous hydrogen pipelines based offshore wind to hydrogen facilities.

The overall optimization problem is quite similar to the previous case, due to the similar route considered for hydrogen produced. The major difference is in the delivery pathway. Therefore, the overall problem statement can be stated as follows. Given a set of demands for hydrogen, a set of candidate offshore locations for siting wind-to-hydrogen facilities and the associated time varying capacity factor for wind power generation, annualized capital and operational costs of investment in technologies used along the process sequence , energy consumption per unit of operation for each process step; design the overall supply chain by selecting one centralized production facility per hub, sizing the facility & determining the capacities required for process steps & schedule the overall operations (production, storage & transport) over the span of a representative year such that the total annualized cost of hydrogen delivery through the system is minimized while adhering to the energy balance constraints, capacity constraints, transportation & storage constraints.

The above optimization problem is also formulated as an MINLP. The mathematical formulation of P2 is as follows:

Objective function

The objective function *obj* shown in Eq. (S25) quantifies total annualized cost of hydrogen delivery through the compressed gaseous hydrogen pipelines based offshore wind to hydrogen facility comprising individual sub-systems such as offshore wind turbines, desalination, electrolysis, compression, storage, and pumping and pipelines. Individual terms represent the TAC of these subsystems, which are obtained by multiplying their unit TAC values (with appropriate units) and corresponding capacities The pipeline costs are modeled based on the hydrogen delivery scenario analysis model (HDSAM)[8] model equations for land based pipelines by assuming a 100% cost increase for sub-sea pipelines. Costs of the hydrogen compressor and pump used for pipeline

transmission, also obtained from HDSAM are subject to non-linear scaling, while other subsystem expenses linearly scale based on their installed capacities. The TAC of each sub-system was obtained from the CAPEX and OPEX costs (See **Methods, Technology costs**).

$$\begin{aligned}\min: \quad obj = & \sum_f \left(TAC^{WT} \cdot N^{f,WT} + TAC^{Des} \cdot C^{f,Des} + TAC^{EL} \cdot C^{f,EL} + TAC^{FLP} \cdot A^{L,EL} \cdot C^{f,EL} \right) \\ & + \sum_f \left(TAC^{:Comp} \cdot C^{f,comp^{\theta^C}} + TAC^{STO} \cdot C^{f,STO} + \sum_d TAC^{:pump} \cdot C^{f,d,pump^{\theta^P}} \right) \\ & + \sum_f \sum_d \left(a e^{\theta^{pipe} \sqrt{A^{f,d,pipe}}} + b A^{f,d,pipe} + c \sqrt{A^{f,d,pipe}} + d \right) \cdot L^{f,d}\end{aligned} \tag{S25}$$

Constraints

Facility selection constraints

The facility selection constraints ensure that a single centralized facility is selected for each hub amongst all the proposed candidate locations. As in the previous case, Eq. (S2) is used to model the restriction of activating only one location in a hub while constraints (S3)-(S5) and (S26) - (S28) employ a set of "Big M" constraints using a large positive constant *M* that ensures the installed capacity of the subsystems are greater than zero only at the location activated for siting in the hub.

$$C^{f,Comp} \leq M \cdot x^f, \qquad \forall f \in F \tag{S26}$$

$$C^{f,STO} \leq M \cdot x^f, \qquad \forall f \in F \tag{S27}$$

$$C^{f,d,pump} \leq M \cdot x^f, \qquad \forall f \in F \tag{S28}$$

Capacity constraints

The capacity constraints ensure that each of the subsystems, which are operating flexibly by adapting to the variable offshore wind energy generation, remain below their respective installed capacities at each time step. Constraint (S10) pertains to desalination, constraint (S11) to electrolysis, constraint (S29) to compression, constraint (S30) to pumping, and constraint (S13) to the storage tank.

$$E_t^{f,comp} \leq C^{f,comp}, \qquad \forall f \in F,\ t \in T \tag{S29}$$

$$E_t^{f,d,pump} \leq C^{f,d,pump}, \qquad \forall f \in F,\ t \in T \tag{S30}$$

Energy balance constraints

In this study, the offshore wind-based hydrogen production facilities are treated as isolated energy systems wherein the entire energy output of the offshore wind farm is exclusively channeled into hydrogen production, devoid of additional storage or external supplementation. Thus, Eq. (S31) establishes the energy balance constraint, ensuring that the total energy demand for hydrogen production aligns with the generation from the

offshore wind turbines at each time step *t*. Eq. (S15) quantifies the energy generation at each time step *t* by multiplying the time-varying wind capacity factor specific to the location (See **Methods, offshore wind energy model**) with the nominal energy output of a single wind turbine, and the total number of installed turbines at facility *f*. Furthermore, Eqs. (S16), (S17), (S32), and (S33) fix the energy requirements for desalination, electrolysis, compression, and pumping, all of which are energy-consuming processes, based on the hydrogen production level at each time step *t*, unit energy consumption parameters, and assumed process efficiencies.

$$E_t^{f,WT} = E_t^{f,Des} + E_t^{f,EL} + E_t^{f,comp} + \sum_d E_t^{f,d,pump}, \qquad \forall f \in F,\ t \in T \tag{S31}$$

$$E_t^{f,comp} = \Phi^{Comp} \cdot F_t^{f,H_2}, \qquad \forall f \in F,\ t \in T \tag{S32}$$

$$E_t^{f,d,pump} = \left(\frac{\Delta P}{l}\right) \cdot \frac{L^{f,d} \cdot M_t^{f,d,H_2}}{\rho^{H_2}}, \qquad \forall f \in F,\ t \in T \tag{S33}$$

Inventory & pipeline sizing constraints

Eq. (S34) applies a dynamic material balance on the storage tank, defining the inventory profile over time. The storage tank receives inputs from the upstream production processes and outputs H_2 to the pipelines. Further, a variation of Eq. (S34) is applied at time-step 0, by replacing the term $L_{t-1}^{f,STO}$ with $L_{364}^{f,STO}$, essentially serving as a cyclicity constraint that enables modeling operating levels across years using a representative 365 day time period. Eq. (S35) imposes the that the maximum flowrate of H_2 at each time period *t* is limited by the designed cross-sectional area of the pipe and the maximum permissible design velocity of the gas.

$$L_t^{f,STO} = L_{t-1}^{f,STO} + F_t^{f,H_2} - \sum_d M_t^{f,d,H_2}, \qquad \forall f \in F,\ t \in T \tag{S34}$$

$$M_t^{f,d,H_2} \le A^{f,d,pipe} \cdot V^{\max} \cdot \rho^{H_2}, \qquad \forall f \in F,\ t \in T,\ d \in D \tag{S35}$$

Demand constraint

The demand satisfaction constraint stipulates that the total hydrogen shipped from all active facilities must be greater than the demand at each receiving coastal location, ensuring adequate supply to meet the specified requirements. Constraint (S36) stipulates that the demand must be met despite losses that occur during the transmission of hydrogen through pipelines by accounting for the pipeline transmission efficiency.

$$\sum_f \sum_t \left(M_t^{f,d,H_2} \cdot \eta^p\right) \le Demand^d, \qquad \forall\ d \in D \tag{S36}$$

The capabilities and structure of the model P2 closely resemble that of the model P1 discussed earlier. The only variations in decisions made through optimization pertain to the delivery pathway. This model sizes pipelines using non-linear variables and determines the time-varying flow rate in these pipelines from the

production facilities to the demand locations, as opposed to selecting ships and scheduling their logistics. Additionally, alongside the concave non-linear terms in the pipeline sizing equations, the capacities of compressors and transmission pumps are assumed to scale non-linearly contributing two additional concave terms. There is also a convex exponential term in the pipeline sizing equation, which is replaced with a piecewise linear approximation. However, similar to the previous case, these non-linearities are present solely within the objective function. For the state-level implementation, P2 contains 2928 variables (2926 continuous & 2 integer) and 4753 constraints.

For the evaluation of the models P1 and P2, spatial offshore wind speed data is used for calculation of the offshore wind capacity factors. The source of this data and the methodology involved are described in section **Methods, Offshore wind energy model**. Additionally, the section **Methods, Hydrogen demand** details the source of the state level hydrogen demand data used in the study. Table S2 outlines the other major parameters essential for the evaluation of the delivered costs of hydrogen through P1 and P2. The results of the optimization models, such as the sub-system sizes and production profiles are used to estimate the lifecycle greenhouse gas emissions of hydrogen. The lifecycle inventory data for offshore wind turbines[9, 10], electrolysis[11-13], liquefaction[14-16], compression[8], shipping[16], and pipelines[8, 17] was sourced from literature and was used in conjunction with the ecoinvent database for the lifecycle assessment.

Table S2. Major input parameters used for the evaluation of the delivered costs of hydrogen for problems P1 & P2.

Parameters	Value	Unit	Ref.
$A^{L,EL}$	0.1	km^2/GW	18
BO	0.1	w% /day	19
C_i^S	1000/10000/14000	t	5
$CapEx^{WT}$	2389	$/kW	20
$CapEx^{EL}$	445	$/kW	21
$CapEx^{DES}$	0.0306	$/ ($m^3$ H_2O/hr)	22, 23
$CapEx^{LIQ}$	6160	$/(kt/hr)	5
$CapEx^{Comp}$	40,035	$/kW	8
$CapEx^{Pump}$	40,035	$/kW	8
$CapEx^{S}$	170/ 500/ 560	MM $	5
$CapEx^{FLP}$	500	MM $/$km^2$	24
h^t	200	m	25
h^m	10	m	26
$L^{f,d}$	100	km	
N^{Days}	365		
$OpEx^{Comp}$	5% $CapEx^{Comp}$	$/kW	8

$OpEx^{LIQ}$	5% $CapEx^{LIQ}$	\$/(kt/hr)	5
$OpEx^{Pump}$	5% $CapEx^{Pump}$	\$/kW	8
$OpEx^{WT}$	70	\$/kW	20
$OpEx^{EL}$	5% $CapEx^{EL}$	\$/kW	27
$OpEx^{DES}$	2.5% $CapEx^{DES}$	\$/kW	22
$P_i^{S,TRA}$	0.05	\$/(kg·km)	5
ρ^{H_2}	42.4	kg/m^3	28
$V^{\max}$	20	m/s	29
W^{Des}	15	L/kg H_2	22
η^{EL}	0.67		4
η^{P}	0.99		
Φ^{WT}	360	MWh	30
Φ^{Des}	3.5	kWh/m^3	22
Φ^{EL}	33.3	kWh/kg H_2	22
Φ^{LIQ}	11.9	kWh/kg H_2	31
Φ^{Comp}	1.35	kWh/kg H_2	32
θ^{L}	0.7983		5
θ^{S}	0.673		5
θ^{C}	0.6038		4
θ^{P}	0.8335		4
θ^{Pipe}	0.0787		4
$v^{w,co}$	25	m/s	25
$v^{w,ci}$	5	m/s	25
$v^{w,r}$	13	m/s	25

Table S3. Input list for the candidate demand locations and offshore facility locations used in the evaluation of the delivered costs of hydrogen for problems P1 & P2.

Hub	Demand Locations - States	Offshore facility locations - Buoy ID
South East	Florida, Georgia ,North Carolina, South Carolina	FWYF1,41002,FPSN7,41002
Lake Eerie	Ohio, Pennsylvania	SBIO1,SBIO1
Michigan Lake	Illinois, Indiana	SGNW3,SGNW3
Superior	Minnesota, Wisconsin, Michigan	PILM4,PILM4,PILM4
West	California, Oregon, Washington	46054,46002,46005
Gulf of Mexico	Alabama, Louisiana, Mississippi, Texas	BURL1,BURL1,BURL1,42002
North East	Connecticut, Delaware, Maine, Maryland, Massachusetts, New Hampshire, New Jersey, New York, Rhode Island, Virginia	ALSN6,ALSN6,MDRM1,44004,BUZM3 ,IOSN3,ALSN6,ALSN6,ALSN6, CHLV2

S4. Computational Performance of the Solution Approach

As described in the section **Methods, Solution approach for global optimization**, MINLP problems featuring separable concave functions in the objective function can be effectively handled by branch-and-refine algorithm[33-35], which uses piece-wise linear approximations of the non-linear terms in the MINLP to sequentially solve a sequence of MILPs. Detailed descriptions of the branch-and-refine algorithm, including pseudocode are provided by Gong et al.[33] and Zhao et al.[34, 35] In this study, the models P1 and P2 described above were implemented using the Pyomo library in Python. SOS-2 type constraints, available through Pyomo, were employed to model the piecewise linear approximations. The commercial MILP solver Gurobi was ultimately utilized for solving the models.

Table S4 summarizes the comparison of the computational performance of adopting the branch-and-refine algorithm versus using open source solvers to directly solve the MINLPs. For this comparison, a state-level implementation of the problems P1 & P2 were used for the state of Alaska. All the computational experiments were performed on a DELL OPTIPLEX 7040 desktop with Intel(R) Core (TM) i7-6700 CPU @ 3.40 GHz and 32 GB RAM. While the open source solvers were able to achieve the optimal solution for the problem P2 in comparable time periods; for the problem P1, they terminated without converging after 86,400 seconds, due to a preset time limit, offering only lower and upper bounds for the solution of problem P1. This difference in performance may be attributed to the significantly higher number of integer variables in P1 as compared to P2. However, for both cases, when the branch-and-refine approach was used, an optimal solution

was obtained in less than 100 seconds. This clearly establishes the advantages of this approach for solving MINLPs with separable concave functions in the objective function.

Table S4. Comparison of computational performance of the branch-and-refine approach versus open source MINLP solvers for problems P1 and P2

Solver	Liquefied Hydrogen Shipping Model (P1)		Compressed Gaseous Hydrogen Pipelines Model (P1)	
	Objective Value	**CPU Run time (s)**	**Objective Value**	**CPU Run time (s)**
Couenne (MINLP)	(1765.61,1878.09)	86,400	1486.78	373
SCIP (MINLP)	(6060.27,6076.91)	86,400	1486.78	1.56
Gurobi (Branch-and-Refine: Reformulated MILPs)	1871.52	62s	1486.78	1.18

References

1. *Pathways to Commercial Liftoff: Clean Hydrogen*, US Department of Energy, 2023.
2. M. F. Ruth, P. Jadun, N. Gilroy, E. Connelly, R. Boardman, A. Simon, A. Elgowainy and J. Zuboy, *The technical and economic potential of the H2@ scale hydrogen concept within the United States*, National Renewable Energy Lab, Golden, CO (United States), 2020.
3. M. Ruth, P. Jadun, E. Connelly, R. Boardman, A. J. Simon, A. Elgowainy, J. Zuboy and N. Gilroy, H2@Scale Concept Hydrogen Demand and Resources [data set], https://doi.org/10.25984/1845000, (accessed 01.04.2023).
4. *National Clean Hydrogen Strategy and Roadmap*, US Department of Energy, 2023.
5. *Global Hydrogen Trade to Meet the 1.5°C Climate Goal Part II : Technology Review of Hydrogen Carriers* IRENA, 2022.
6. P. Belotti, P. Bonami, M. Fischetti, A. Lodi, M. Monaci, A. Nogales-Gómez and D. Salvagnin, *Computational Optimization and Applications*, 2016, **65**, 545-566.
7. T. Blanke, K. S. Schmidt, J. Göttsche, B. Döring, J. Frisch and C. van Treeck, *Energy Informatics*, 2022, **5**, 1-14.
8. K. Reddi, A. Elgowainy, N. Rustagi and E. Gupta, *Int. J. Hydrogen Energy*, 2017, **42**, 21855-21865.
9. C. Li, J. M. Mogollón, A. Tukker, J. Dong, D. von Terzi, C. Zhang and B. Steubing, *Renew. Sustain. Energy Rev.*, 2022, **164**, 112603.
10. C. Li, J. M. Mogollón, A. Tukker and B. Steubing, *Environmental Science & Technology*, 2022, **56**, 11567-11577.
11. K. Bareiß, C. de la Rua, M. Möckl and T. Hamacher, *Appl. Energy*, 2019, **237**, 862-872.
12. S. Lundberg, *Comparative LCA of Electrolyzers for Hydrogen Gas Production*, KTH Royal Institute of Technology, 2019.
13. S. Evangelisti, C. Tagliaferri, D. J. Brett and P. Lettieri, *J. Clean. Prod.*, 2017, **142**, 4339-4355.
14. K. Stolzenburg and R. Mubbala, *Integrated design for demonstration of efficient liquefaction of hydrogen (IDEALHY), FCH JU*, 2013.
15. H. Kim, J. Haider, M. A. Qyyum and H. Lim, *J. Clean. Prod.*, 2022, **367**, 132947.
16. S. Kolb, J. Müller, N. Luna-Jaspe and J. Karl, *J. Clean. Prod.*, 2022, **373**, 133289.
17. C. Tsiklios, M. Hermesmann and T. Müller, *Appl. Energy*, 2022, **327**, 120097.
18. P. Ripson and H. v. Noordende, *A One-GigaWatt Green-Hydrogen Plant: Advanced Design and Total Installed-Capital Costs*, Hydrohub Innovation Program, 2022.
19. Kawasaki Completes Basic Design for World's Largest Class (11,200-cubic-meter) Spherical Liquefied Hydrogen Storage Tank,

https://global.kawasaki.com/en/corp/newsroom/news/detail/?f=20201224_8018, (accessed 27.11.2023).
20. M. Shields, P. Beiter and J. Nunemaker, *A Systematic Framework for Projecting the Future Cost of Offshore Wind Energy*, National Renewable Energy Laboratory, Golden, CO (United States), 2022.
21. IEA, Global Energy and Climate Model 2023 key input data, https://www.iea.org/data-and-statistics/data-product/global-energy-and-climate-model-2023-key-input-data, (accessed 27.11.2022).
22. A. Singlitico, J. Østergaard and S. Chatzivasileiadis, *Renewable and Sustainable Energy Transition*, 2021, **1**, 100005.
23. *The Future of Hydrogen*, IEA, 2019.
24. M. Jansen, C. Duffy, T. C. Green and I. Staffell, *Advances in Applied Energy*, 2022, **6**, 100090.
25. T. R. Lucas, A. F. Ferreira, R. S. Pereira and M. Alves, *Appl. Energy*, 2022, **310**, 118481.
26. National Data Buoy Center, Historical NDBC Data, https://www.ndbc.noaa.gov/historical_data.shtml, (accessed 21.04.2023).
27. A. Bose, N. Lazouski, M. L. Gala, K. Manthiram and D. S. Mallapragada, *ACS Sustain. Chem. Eng.*, 2022, **10**, 7862-7872.
28. Hyrdogen Tools, Hydrogen Density at different temperatures and pressures, https://h2tools.org/hyarc/hydrogen-data/hydrogen-density-different-temperatures-and-pressures, (accessed 27.11.2023).
29. N. González Díez, *WP1E – Impact of high speed hydrogen flow on system integrity and noise*, HyDelta, 2021.
30. *Definition of the IEA 15-Megawatt Offshore Reference Wind*, National Renewable Energy Laboratory, Golden, CO (United States), 2020.
31. S. Z. Al Ghafri, S. Munro, U. Cardella, T. Funke, W. Notardonato, J. M. Trusler, J. Leachman, R. Span, S. Kamiya and G. Pearce, *Energy Environ. Sci.*, 2022, **15**, 2690-2731.
32. M. Gardiner, *Energy requirements for hydrogen gas compression and liquefaction as related to vehicle storage needs*, U.S. Department of Energy, 2009.
33. J. Gong and F. You, *ACS Sustain. Chem. Eng.*, 2015, **3**, 82-96.
34. X. Zhao and F. You, *ACS Sustain. Chem. Eng.*, 2021, **9**, 12167-12184.
35. X. Zhao and F. You, *AlChE J.*, 2021, **67**, e17127.